Steady-State Critical Heat Flux in Water-Cooled Reactor Fuel Elements

F. Mayinger

The basic aspects of critical heat flux in forced convective flow were already discussed in detail in Chap. 8 and the nomenclature for critical heat flux condition was given as

Burnout—a physical destruction of the heated surface
DNB—departure from nucleate boiling
Dryout—an expression for an unwetted spot at the heated surface

All these expressions are unsatisfactory for a general description of the phenomenon, therefore Collier (1972) chose the term "critical heat flux condition" to denote the state of the system when the characteristic reduction in heat transfer coefficient has just occurred and the term "critical heat flux" to describe the value of heat flux at which, and local to the point at which, this state of the system first occurs. Sometimes the term "boiling crises" also is used to describe the critical heat flux condition.

As pointed out by Hewitt, critical heat flux conditions in forced convective flow are dependent on a large number of geometric, thermodynamic, and hydrodynamic parameters. There is, for example, the influence of the channel cross-section, of quality, of mass flow rate, and of the history of the flow downstream to the local spot where a DNB or dryout takes place. In general, we have to distinguish between critical heat flux condition at low and high or medium steam qualities. In a nuclear reactor we have, in addition to the basic problems of the critical heat flux conditions:

a nonuniform heating of the rods
a noncircular geometry

equipment to hold the rods of a cluster in the correct distance, e.g., grid-type spacers
radial mixing between subchannels and unsteady thermohydraulic conditions

All these additional influences have to be taken into account if one tries to predict the critical heat flux in a water-cooled reactor, or if one wants to correlate studies done in simple geometries and with uniform heat flux distribution with the limitations of the critical heat flux in nuclear reactor design.

1 NONUNIFORM AXIAL HEAT FLUX PROFILE

Before discussing briefly the influence of the heat-flux shape, we recapitulate the flow conditions in the two-phase mixture being present at the onset of the boiling crisis, i.e., whether we have low or high steam quality. In general, one will realize that the critical heat flux will become smaller with growing steam quality. Figure 1 shows the principal differences of the flow behavior. At low

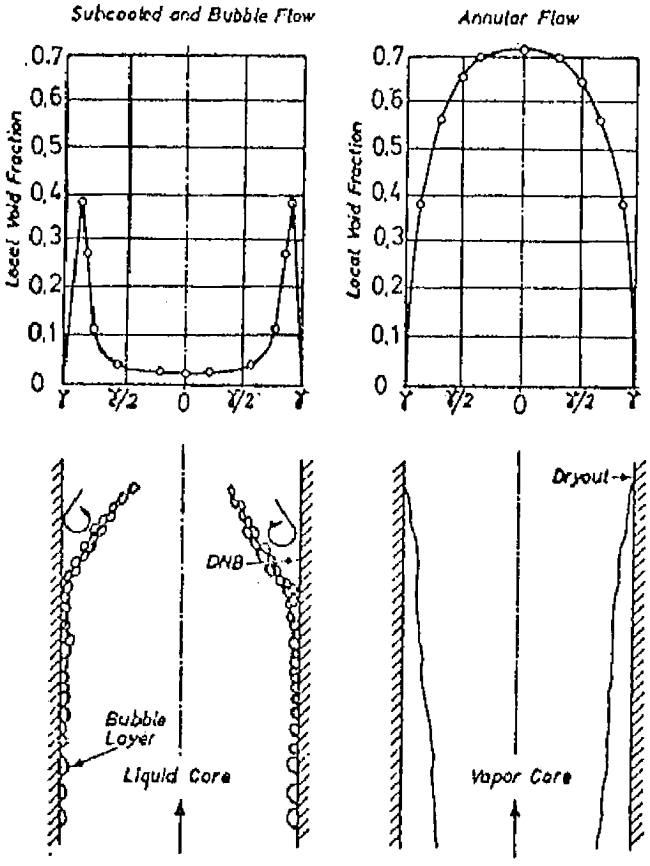

FIG. 1 DNB and dryout occurrence (from Tong, 1965).

quality or at subcooled boiling, so many bubbles originate near the wall that the heat cannot be completely transported from the wall because the superheated liquid layer between the wall and the bubbles vaporizes. Between the liquid flow in the center of the channel and the wall, therefore, an insulating steam layer is formed. To create this condition, a very high heat flux density is necessary. These conditions are given in the left side of Fig. 1 where, in the upper part, the local void fraction versus the channel cross-section is plotted and, in the lower part, the flow behavior of the bubbles is demonstrated.

Quite different from this behavior are the critical heat flux conditions in an annular flow that are present at medium and high steam quality. As shown on the right-hand side of Fig. 1, there is a thin liquid film at the wall which, due to the evaporation and entrainment, slowly becomes thinner and, finally, locally may disappear; this is called dryout. Because of the fact that, with dryout, the critical heat flux is lower than with DNB and, because of higher steam velocities the heat transfer coefficient after the dryout reaches a certain amount, the temperature rise at the wall usually is slower with dryout than with DNB.

2 NONUNIFORM HEAT FLUX DISTRIBUTION

In nuclear reactors, the form of the heat flux axial profile often resembles a given sine wave

$$\phi(z) = \phi_{\max} \sin\left(\frac{\pi z}{L}\right) \tag{1}$$

The simplest way to predict the critical heat flux behavior of a fuel rod with sine heat flux distribution would be to assume that the critical heat flux condition is dependent only on the local parameters at the burnout spot and to use a semigraphical method, as shown in Fig. 2. If we knew a critical heat flux correlation of the form, for example

$$\phi_{\text{crit}} = f[G_1 i(z)_1 p_1 D_1 z]_i \tag{2}$$

or

$$\phi_{\text{crit}} = f[G_1 \dot{x}(z)_1 p_1 D_1 z]_i \tag{3}$$

we could plot the local critical heat flux as a function of the quality $\dot{x}$, the channel length z, or the local enthalpy i of the fluid, as done in Fig. 2. In addition, we can add to this figure the real heat flux distribution over the channel length or expressed in terms of the local quality or the local enthalpy in the channel. It can easily be seen from this figure that the boiling crisis

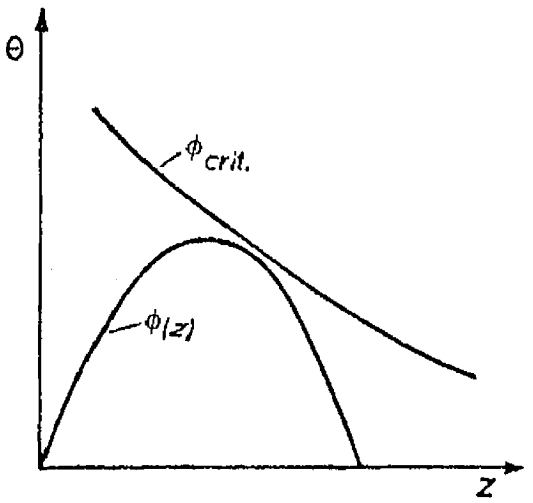

FIG. 2 Local critical heat flux and heat flux profile.

there occurs where the curve for the real heat flux distribution of the rod, and the curve predicting the local critical heat flux are touching each other. Using this simple method would mean that only the heat- and the energy-balance upstream of the burnout spot are influencing critical heat flux conditions and that there is no "memory effect" for flow distribution, boundary layer effects, and so on. More quantitatively, we can handle the problem in the following way.

If it is assumed that there is a unique relationship between critical heat flux and local mass quality, then the case of a nonuniformly heated tube can be dealt with, as just mentioned, in a straightforward manner. Empirical correlations predicting critical heat flux were already discussed in Chap. 2. Probably one of the simplest but also most general empirical correlations is the equation of Macbeth (1963), assuming that the critical heat flux is a linear function of quality, thus

$$\phi_{\text{crit}} = A - B\dot{x}(z)i \tag{4}$$

where A and B are assumed to be functions of mass flow rate pressure and equivalent diameter. For the case of such a linear form of the relationship, the operation predicting local critical heat flux is very simple and has been formulated in detail by Barnett (1964). The distance along the tube is denoted by z, the functional form of the heat flux profile by $f(z)$, the local heat flux by $\phi(z)$, and the peak heat flux by $\phi_{\max}$.

$$\phi(z) = \phi_{\max} f(z)i \tag{5}$$

The mean enthalpy of the steam-water mixture at a distance z is given by

$$i(z) - i_l = \frac{4\phi_{max}}{DG}\left(\int_0^z f(z)\,dz\right) - (\Delta i_{sub})_l \tag{6}$$

The Macbeth form of the linear critical heat flux versus quality relationship can be written in terms of the local enthalpy as

$$\phi_{crit}(z) = A - CDG\frac{i(z) - i_l}{4i} \tag{7}$$

The critical heat flux will occur at z when $\phi(z)$ and $i(z)$, related by Eq. (6), also satisfy Eq. (7). If $(\phi_{max})_{crit}(z)$ is the value of the peak heat flux when the critical heat flux is exceeded at z, then

$$(\phi_{max})_{crit}(z) = \frac{4A + DGC(\Delta i_{sub})_l}{4\left[f(z) + C\int_0^z f(z)\,dz\right]}i \tag{8}$$

Equation (8) gives the predicted value of the heat flux when the critical heat flux first occurs at a distance z from the inlet, regardless of whether it has occurred elsewhere in the system. Clearly, the predicted first occurrence of the critical condition as the total power applied to the tube is increased will correspond to the lowest value of $(\phi_{max})_{crit}(z)$. As given by Eq. (8), this will be when

$$\frac{d}{dz}\left[f(z) + C\int_0^z f(z)\,dz\right] = 0 \tag{9}$$

Using values of A and C derived from data taken from uniformly heated tube, Barnett (1964) compared the predictions of Eq. (8) with experimental data from Lee and Obertelli (1963) and Lee (1965).

Predicted values of the peak heat flux were consistently higher than the experimental values. The accuracy of the prediction varied considerably with pressure. The method did, however, appear satisfactory to predict the area of the tube over which the critical condition would occur. This comparison showed that the "local conditions" hypothesis is not generally valid. Another proposed method for predicting DNB with nonuniform heat flux is the "overall power" hypothesis. Its basic idea is that the total power, $\int_{z_0}^{z_{DNB}} Ugdz$, added to the fluid from the point where, for the first time, the bubbles detach from the wall up to the DNB spot, is the same for uniform and nonuniform heat flux distribution. Expressed in terms of enthalpy, we can write

critical heat flux for a uniform heat flux profile is obtained. From the definition of F, it follows that

$$[\phi_{crit}(z)]_{nu} = \frac{A + CD[G(\Delta i_{sub})_i/4]}{F + C\int_0^{z_{crit}} [\phi(z)/\phi(z_{crit})]\, dz}\, i \tag{13}$$

The ratio $\phi(z)/\phi(z_{crit})$ in Eqs. (12) and (13) may be replaced by $f(z)/f(z_{crit})$; thus, both integrals are functions of the flux profile only and can be evaluated directly as a function of z_{crit}. The value of the factor has been determined by fitting the method to experimental data. Tong found that Ω is a function of both local steam quality, $x(z_{crit})$, and mass velocity, G, thus

$$\Omega = 0.44\, \frac{[1 - x(z_{crit})]^{7.9}}{(G/10^6)^{1.72}}\, i \quad (\text{in.}^{-1}) \tag{14}$$

where the mass velocity is given in lb/hr-ft^2. Lee found, when correlating a large number of nonuniform critical heat flux data, that Ω was well represented by

$$\Omega = \frac{k\delta}{D(\phi_{max}/\bar{\phi})}\, i \quad (\text{in.}^{-1}) \tag{15}$$

where k is a constant dependent on pressure, as given in Table 1, and δ is the dimensionless axial flux gradient taken at the point of average flux in the upper part of the tube.

$$\delta = \frac{d[\phi(z)/\bar{\phi}]}{d(z/D)} \quad \text{at} \quad \frac{\phi(z)}{\bar{\phi}} = 1 \tag{16}$$

The deliberations up to now did not treat the spot at which DNB occurs, but purely the region up to this spot. Another complete deliberation is presented in the so-called "boundary layer" model. A forming of a vapor layer at the wall means that the liquid is displaced from the wall. But this displacing, or forming, of the vapor layer cannot be calculated with the well known boundary-layer theory; on the contrary, one has to evaluate this with the help

TABLE 1 Optimized values of k

Pressure (psia)	560	1000	1250	1550	1800	2000
Bar	38.6	69	86	107	124	138
k	3.67	5.00	3.98	3.59	2.48	1.03
RMS error (%)	3.96	7.18	8.8	5.78	5.27	8.30

of measurements. This was done by injecting isothermal vapor through a porous wall and, empirically, the following correlation was found.

$$(\rho_g U_g)_{\text{crit}} = \frac{\xi}{2} \rho_f U_f \tag{17}$$

In this equation, ξ is the flow resistance factor for the flow without injecting steam through the wall. If we replace the superficial steam velocity, U_g, in Eq. (17) by the heat flux density and the latent heat of evaporation, we get

$$\frac{\phi_{\text{DNB}}}{i_{fg}} = \frac{\xi}{2} \rho_f U_{fi} \tag{18}$$

or, rearranged

$$\phi_{\text{DNB}} = \frac{\xi}{2} i_{fg} \rho_f U_{fi} \tag{19}$$

For the flow resistance factor, ξ, we can use the well known values from the literature.

Comparing this procedure with the "F-model," we easily can see that the boundary-layer model does not take into account the memory effect and, therefore, especially in the subcooled region, it is much less accurate.

At medium and high qualities there is annular flow in the heated channel. Therefore, a liquid layer exists at the wall, whereas the vapor flows in the center of the channel. The steam carries liquid droplets with it. Calculating the critical heat flux in such a flow regime, one generally regards only the liquid which can–as mentioned–be present in the film at the wall and in the form of droplets in the vapor core. Furthermore, one defines as "entrainment" the droplets that are carried in the vapor and as "deposit" the droplets leaving the vapor core and falling onto the liquid at the wall. One also can easily imagine that the relationship between entrainment and deposit influences the critical heat flux. The mechanism of entraining the liquid layer already was explained in great detail elsewhere and will not be repeated here.

3 EMPIRICAL CORRELATIONS

Numerous correlations can be found in the literature for predicting critical heat flux. They could be subdivided simply into equations on a more theoretical basis and those which are purely empirical correlations. But we also can distinguish between the DNB- and the dryout-behavior. A really theoretical attempt for critical heat flux correlations with forced convective flow is made only in the dryout-controlled critical heat flux, as demonstrated by Hewitt.

In the face of these numerous correlations, one has to make a selection for their presentation. This selection may be influenced by a very practical reason by asking which are the correlations used by the vendors or the manufacturers of nuclear power plants. Here we have to mention mainly three equations; namely, the correlations of

General Electric (also called Jansen Levy equation)
Westinghouse (also called W-3 correlation)
Babcock & Wilcox (also called B and W-2 correlation)

These equations are shown in Table 2, together with their range of validity. In addition, there are also presented in Table 2 other burnout correlations that stand out by their simplicity combined with noteworthy accuracy. These are the equations given by Macbeth and by Barnett, which also are used in the layout of nuclear power plants by different vendors.

In the Macbeth equation, it is assumed that there is a linear relationship between the critical heat flux, the equivalent diameter, the mass flow rate, and the enthalpy rise in the heated channel. More correctly, perhaps one should say that there is, in addition, a nonlinear correction for mass flow rate and equivalent diameter given in the factor A.

The Jansen Levy correlation is used mostly for the geometrical configurations given in boiling-water reactors only and is subdivided into three equations, depending on the steam quality. The most complex form is to be found with the Westinghouse W-3 correlation. There is a special correction function for nonuniform heat flux distribution which has to be integrated from the beginning of the heated length up to the DNB point. This equation preferably should be used when the critical heat flux is DNB-controlled. The nonuniform heat flux distribution is taken in account by the F-correction factor which was discussed in Chap. 2.

More theoretically based approaches in recent times are mainly done for dryout-controlled critical heat flux. A relatively simple approach to calculate the net droplet transfer in the film is to assume a linear relationship as follows

$$E - D = k(w_{LF} - w_{LF\infty})_l \tag{20}$$

where E is the rate of entrainment, D the rate of deposition per unit of channel wall surface, W_{LF} the actual film flow, and $W_{LF\infty}$ the film flow for "hydrodynamic equilibrium," where the entrainment rate would equal the deposition rate. k is a proportionality factor which would be expected to depend on system parameters.

The simple linear approach given in Eq. (20) was used by Anderson (1972) in deriving a film-flow model, and he found that reasonably good fits to burnout data could be obtained by taking the value of k proportional to the square root of the ratio of the vapor to liquid density. He calculated W_{LF}

TABLE 2 Empirical Correlations

Westinghouse W-3 (all walls heated)

$$\frac{q''_{\mathrm{DNB,EU}}}{10^6} = \{(2.022 - 0.0004302P) + (0.1722 - 0.0000984P)$$
$$\times \exp[(18.177 - 0.004129P)x]\}$$
$$\times [(148 + 596x + 0.1729x|x|)G/10^6 + 1.037]$$
$$\times [1.157 - 0.869x] \times [0.2664 + 0.8357 \exp(-3.151D_e)]$$
$$\times [0.8258 + 0.000794(H_{\mathrm{sat}} - H_{\mathrm{in.}})]$$

Nonuniform heat flux

$$q''_{\mathrm{DNB,N}} = \frac{q''_{\mathrm{DNB,EU}}}{F}$$

$$F = \frac{C}{q''_{\mathrm{local}}[1 - \exp(-CL_{\mathrm{DNB,EU}})]} \int_0^{L_{\mathrm{DNB}}} q''(z) \exp[-C(L_{\mathrm{DNB,N}} - z)]\, dz$$

$$C = 0.44 \frac{(1 - x_{\mathrm{DNB}})^{7.9}}{(G/10^6)^{1.72}} \quad (\mathrm{in.}^{-1})$$

W-3 correlation for uniform heat flux distribution for unheated walls

$$\frac{q''_{\mathrm{DNB\ unheated\ walls}}}{q''_{\mathrm{DNB,EU}}(D_e \text{ is to be replaced by } D_h)} = (1.36 + 0.12e^{9x})(1.2 - 1.6e^{-1.92D_h})(1.33 - 0.237e^{5.65x})$$

$$P = \frac{1000}{2300} \quad (\mathrm{psia})$$

$$G = \frac{1.0 \times 10^6}{5.0 \cong 10^6} \quad [\mathrm{lb/(ft^2)(hr)}]$$

$$D_e = \frac{0.2}{0.7} \quad (\mathrm{in.})$$

$$x_{\mathrm{loc}} \leqq |0.15|$$

$$H_{\mathrm{in.}} \geqq 400 \quad (\mathrm{Btu/lb})$$

$$L = \frac{10}{144} \quad (\mathrm{in.})$$

$\frac{\text{Heated}}{\text{Wetted}}$ perimeter = 0.88 — 1.0

$q''_{\mathrm{DNB,EU}}$ = CHF for uniform distribution [Btu/(hr)(ft²)]

$q''_{\mathrm{DNB,N}} = q''_{\mathrm{crit}}$ nonuniform heat flux distribution

L_{DNB} = axial DNB length (in.)

D_e = equivalent diameter, referred to wetted perimeter (in.)

D_h = equivalent diameter, referred to heated perimeter (in.)

Barnett

$$q''_{crit} = 10^6 \left[\frac{A + B(H_L - H_{in.})}{C + L} \right]$$

$$A = 67.45 D_{HE}^{0.68} \left(\frac{G}{10^6} \right)^{0.192} \left[1 - 0.744 \exp - 6.512 D_{HY} \left(\frac{G}{10^6} \right) \right]$$

$$B = 0.2587 D_{HE}^{1.261} \left(\frac{G}{10^6} \right)^{0.817}$$

$$C = 185.0 D_{HY} 1.415 \left(\frac{G}{10^6} \right)^{0.212}$$

$$D_{HE} = \frac{D_o^2 - D_I^2}{D_I}$$

$$D_{HY} = D_o - D_I$$

$L = 24$–108 (in.)

$P = 1000$ psia

$G = 0.14$–6.2×10^6 [lb/(hr)(ft²)]

$H_{in} = 0$–412 (Btu/lb)

$0.258 \text{ in.} < D_{HE} < 3.792$

$0.127 \text{ in.} < D_{HY} < 0.875$

$D_I = \text{Drod}$ (rod diameter) (in.)

$D_o = [\text{Drod}\,(\text{Drod} + D^*_{HE})]^{1/2}$

$$D^*_{HE} = \frac{4(\text{cross section of flow})}{4.5\ \text{Drod}}$$

$$S = \sum_{\text{rods}} \frac{q''_{rod}}{q''_{max}}$$

MacBeth

$$q''_{crit} = 10^6 \left[\frac{A + 0.25 D_e (G/10^6)(H_L - H_{in.})}{B + L} \right]$$

$$A = 67.6 D_e^{0.83} \left(\frac{6}{10^6} \right)^{0.57}$$

$$B = 47.3 D_e^{0.57} \left(\frac{6}{10^6} \right)^{0.27}$$

rod diameter = 0.2–0.55 (in.)

length $L = 36$–72 (in.)

hydr. diameter D_e (in.)

pressure = 1000 (psia)

$G = 0.18$–4×10^6 [lb/(ft²)(hr)]

$H_{in} = 0$–283 (Btu/lb)

q''_{crit} [Btu/(hr)(ft²)]

TABLE 2 Empirical correlations (*Continued*)

Healzer, Hench, Jansen, Levy

$$q''_{crit} = 10^6\left[1.1 - 0.1\left(\frac{P-600}{400}\right)^{1.25}\right] \quad \rightarrow \text{for } x < x_1$$

$$q''_{crit} = [1.9 - 3.3x - 0.7\tanh^2(3\times10^{-6}G)] \times \left[1.1 - 0.1\left(\frac{P-600}{400}\right)^{1.25}\right]10^6 \quad \rightarrow \text{for } x_1 < x < x_2$$

$$q''_{crit} = [0.6 - 0.7x - 0.09\tanh^2(2\times10^{-6}G)] \times \left[1.1 - 0.1\left(\frac{P-600}{400}\right)^{1.25}\right]10^6 \quad \rightarrow \text{for } x_2 < x < x_3$$

$$x_1 = 0.273 - 0.212\tanh^2(3\times10^{-6}G)$$

$$x_2 = 0.5 - 0.269\tanh^2(3\times10^{-6}G) + 0.0346\tanh^2\times(2\times10^{-6}G)$$

$$x_3 = 0.657 - 0.1286\tanh^2(2\times10^{-6}G)$$

$P = 600$–1450 (psia)

$G = 0.2$–16×10^6 [lb/(ft²)(hr)]

q''_{crit} (in.) [Btu/(hr)(ft²)]

Babcock, Wilcox B & W-2

$$q''_{DNB,EU} = \left\{\frac{1.15509 - 0.40703D_e}{(12.710)\left[3.0545\left(\frac{G}{10^6}\right)\right]^A}\right\} \times \left\{(0.3702\times10^6)\left[0.59137\left(\frac{G}{10^6}\right)\right]^B - 0.15208x_{crit}H_{fg}G\right\}$$

$$A = 0.71186 + (0.20729\times10^{-3})(p - 2000)$$

$$B = 0.8340 + (0.68479\times10^{-3})(p - 2000)$$

$$F = \frac{q''_{DNB,EU}}{q''_{DNB,N}}$$

$$F = \frac{1.025C\int_0^{L_{DNB}} q''(z)\exp[-C(L_{DNB,N} - z)]\,cz}{q''_{local}[1 - \exp(CL_{DNB,EU})]}$$

$$C = \frac{0.249(1 - X_{DNB})^{7.02}}{(G/10^6)^{0.637}}$$

$D_e = 0.2$–0.5 (in.)

$P = 2000$–2450 (psia)

$G = 0.95\times10^6 - 40\times10^6$ [lb/(ft²)(hr)]

$X = -3\%$–$+22\%$

$\left.\begin{matrix} q''_{DNB,EU} \\ q''_{DNB,N} \end{matrix}\right\}$ look $w - 3$

from two-phase pressure-drop correlations by employing a so-called triangular relationship for annular flow coupled with an interfacial roughness correlation. The difficulty with the linear approach to film-flow modeling is that data for k are not generally available and, in any case, the use of a linear expression may not be correct, particularly when there are large departures from equilibrium.

More sophisticated models for burnout in annular flow have been developed by Whalley et al. (1973), by Hutchinson et al. (1973), and by Sursock (1973). This short literature survey is given only to enable the reader to inform himself about the newest developments in the literature concerning dryout-modeling.

4 SPECIAL INFLUENCES

The rods in the core of a nuclear reactor are held in position at the bottom and at the top by gridplates, and in between, at a distance of about every 0.5 m, by spacers. These spacers cause an additional pressure drop and also influence the critical heat flux behavior. In boiling-water reactors, the spacers sometimes are designed in such a manner that they improve the mixing between the bubble layer and the liquid near the wall, especially with subcooled boiling or at low qualities. In boiling-water reactors, the influence of spacers is not so evident. Generally speaking, it is possible to enlarge the critical heat flux by a suitable design of the spacers. One possible form is the so-called twisted-tape spacer. This form would improve the droplet disposition and so would enlarge the critical heat flux. But due to other—mainly mechanical and metallurgical—drawbacks, up to now it has not been used.

Another serious problem is the mixing between subchannels. The power density over the cross-section of the core is nonuniform and the rods, therefore, have a different heat flux density. This may result—mainly but not only in boiling-water reactors—in a difference of steam quality between two adjacent subchannels that are formed, for example, between six rods. Measurements have shown that there is a strong mixing and so, an enthalpy and quality exchange between the subchannels, which influences the critical heat flux very strongly. So, before calculating the critical heat flux behavior, one has to do a subchannel-mixing analysis as presented by Rouhani in his referat.

Furthermore there are—mainly in boiling-water reactors—so-called cold- and hot-wall effects. The influence of these effects may be different, depending on whether there is subcooled or low-quality boiling, or whether dryout prevails.

Discussion of some experimental results (Hein and Kastner, 1972) illustrates some special influences resulting from spacers, from nonuniform radial heat flux distribution, and from transient conditions. Spacers can diminish the critical heat flux as well as improve it, depending from their hydrodynamic behavior. It is easy to understand that their influence increases

with growing mass flow rate. The temperature traces of the oscillograph in Fig. 3 show that, at low mass flow rates, the burnout always occurred at the end of the test section, while with mass flow rates of 100 g/cm^2-s, the temperature first rose immediately behind the spacer. The hot spot behind the spacer is demonstrated in the lower part of Fig. 3. This is an example of where the "flow shadow" behind the spacer caused a hot spot.

In an axial uniformly heated rod bundle, the spacer causes more and more influence the nearer its position to the upper end of the rods, as seen in Fig. 4. From this figure it also seems to be evident that, with larger radial hot-channel factors, the effect of the spacer disappears more and more. But it is questionable whether the spacer—due to its design—promotes the mixing or not.

If there is not a special mixing effect due to the spacer, the critical heat flux in a rod bundle with spacers usually is lower than without them. This diminution can amount to as much as 20%, as seen in Fig. 5, where two spacer designs are compared. Both spacers shown in this figure are not used in nuclear reactors; they just served for fundamental research.

In single-phase heat transfer, better heat transfer coefficients usually have to be paid for with higher fanning factors, that is, with higher pressure drop. This is not essentially the same with critical heat flux and boiling. Figure 6 shows that the spacer with the worse DNB behavior also has the higher pressure drop.

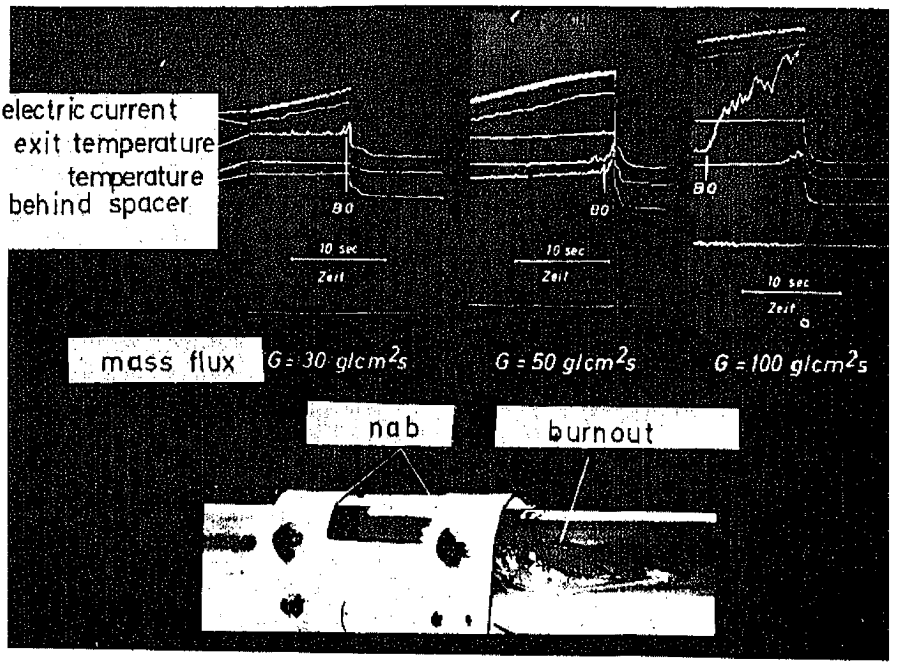

FIG. 3 Burnout temperature traces behind a spacer (above); influence of mass flow rate (below).

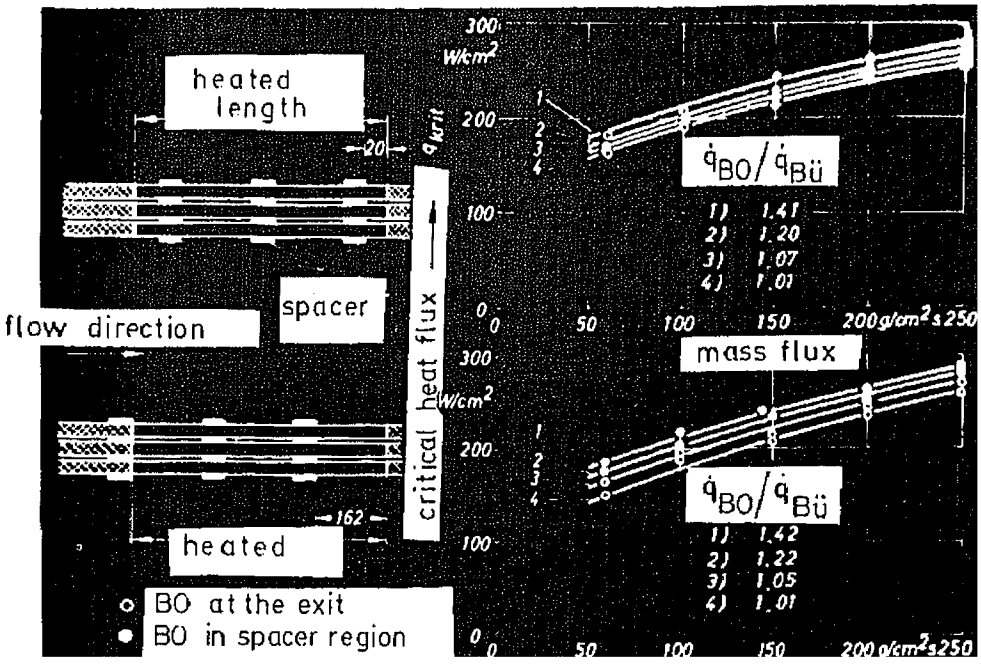

FIG. 4 Influence of the spacer position.

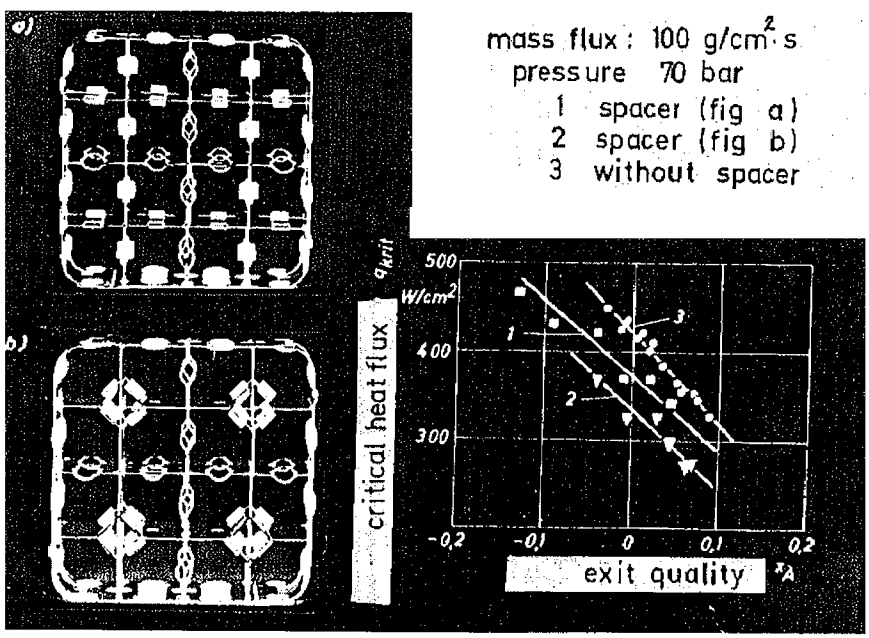

FIG. 5 Influence of spacer design on critical heat flux.

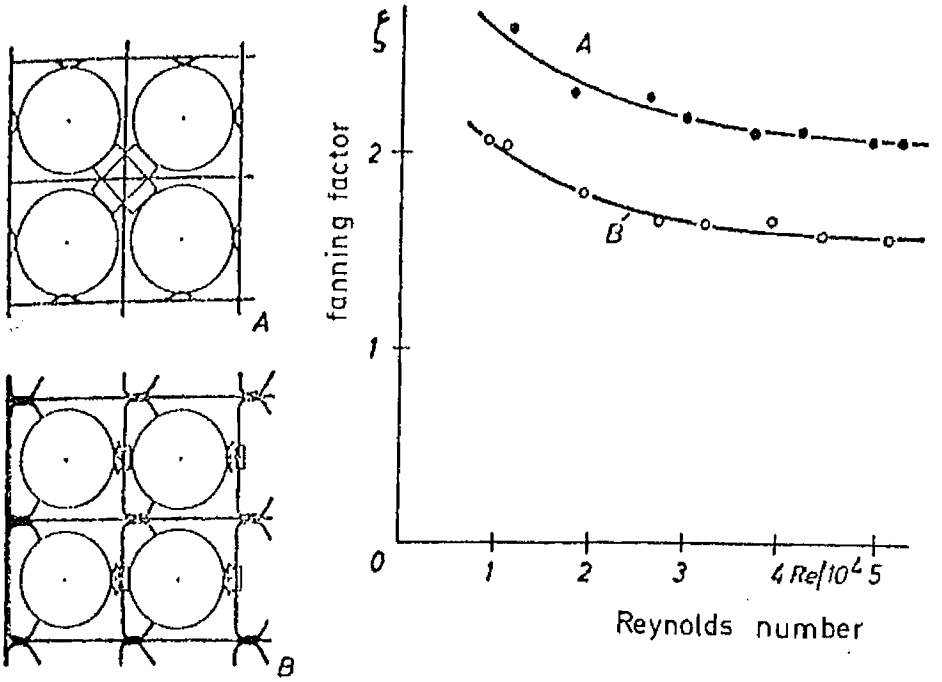

FIG. 6 Fanning factors of special spacer design.

A real improvement in the critical heat flux can be achieved only by spacers that induce artificial mixing. In the most simple design, this can be done by fastening small twisted tapes at the downstream end of the spacer in the free open area formed by each four rods, as shown in Fig. 7.

But the area of the influence downstream from the spacer is limited, due to the friction forces which damp out the artificially induced mixing flow. Thus, the improvement in critical heat flux is small compared to the metallurgical difficulties and design problems arising from this construction. Metallurgical problems are due mainly to corrosion and vibration of the twisted tapes.

Due to control rods or wall effects in the core of the reactor, there is always a more or less uneven radial heat flux distribution. Tests showed that this may influence the critical heat flux quite strongly. In Fig. 8, experimental results measured in a 9-rod bundle are shown. The test rod in this bundle was the center rod, which always was heated until the boiling crises occurred. During each test, the surrounding 8 rods were kept at constant heat flux, which was varied from test to test between 0 and 90 W/cm^2. Such different hot-channel factors could be imitated. Compared to the real conditions in a nuclear reactor, these factors certainly were much too high, but the purpose of these tests was to demonstrate the influence of the hot-channel factor as clearly as possible. Results of tests with more realistic heat flux distribution are shown in Fig. 9, performed in a 4-rod cluster.

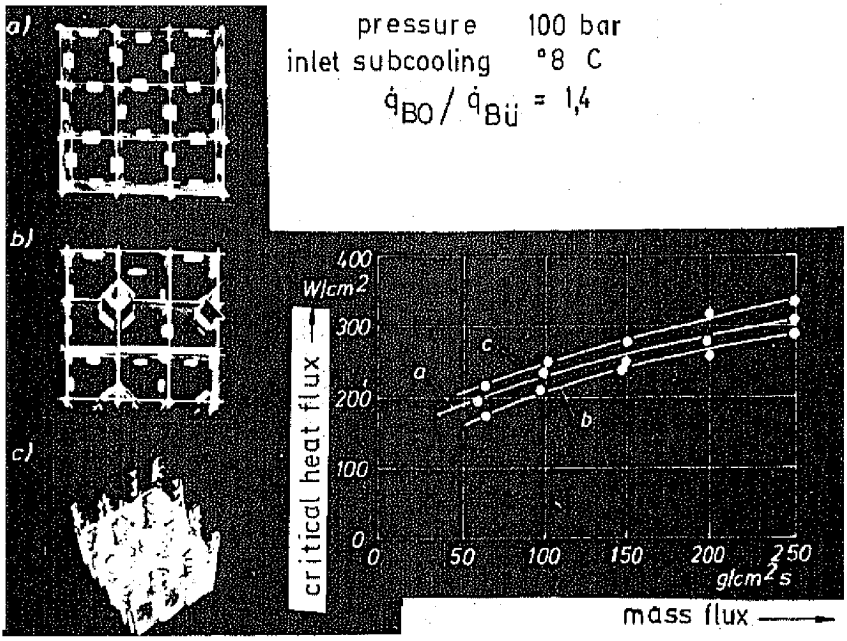

FIG. 7 Influence of spacers and twisted tapes on critical heat flux.

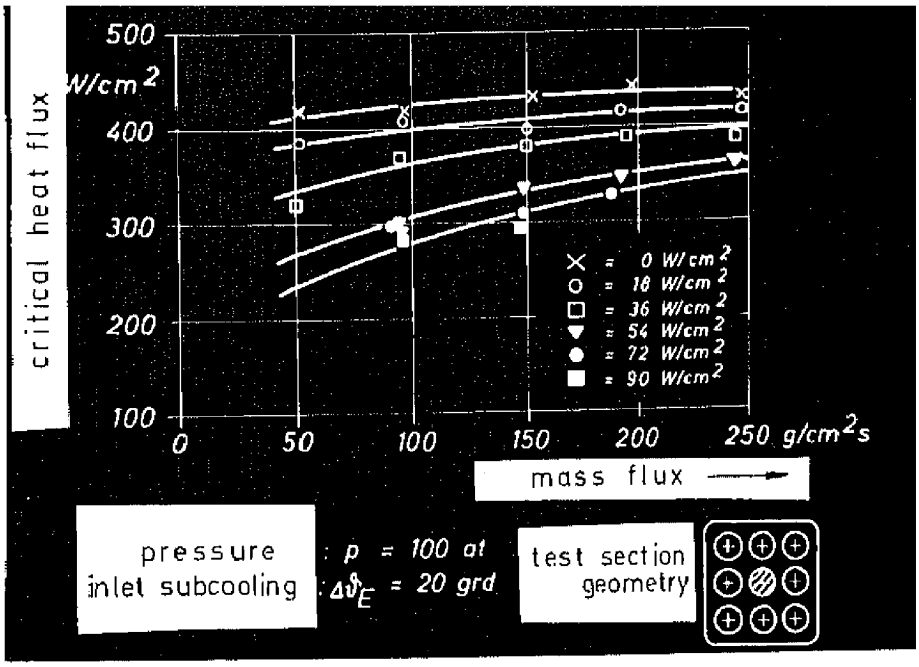

FIG. 8 Critical heat flux with radial nonuniform power distribution, 9-rod bundle.

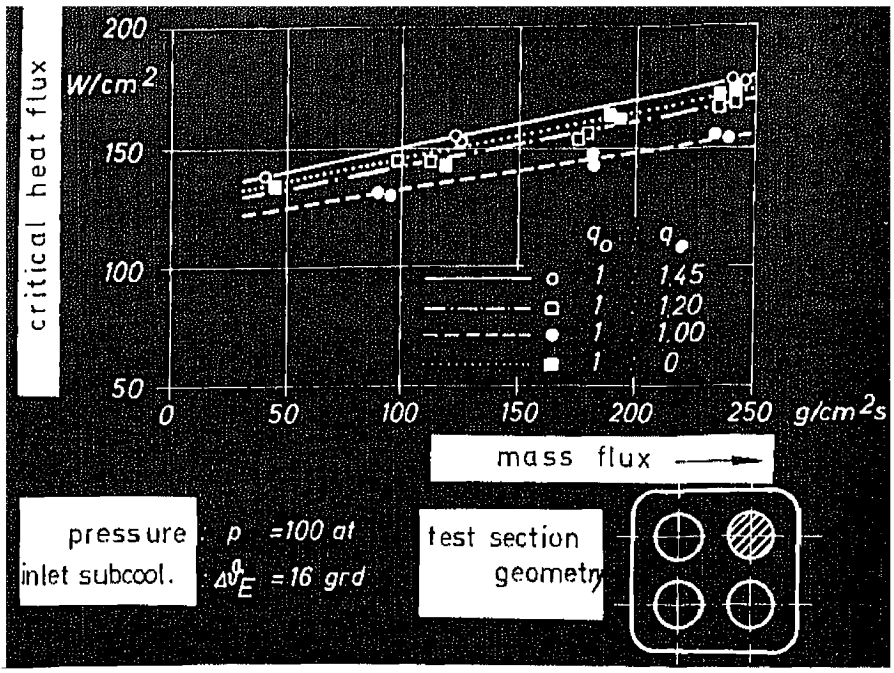

FIG. 9 Critical heat flux with radial nonuniform power distribution, 4-rod bundle.

Looking at these results, it is clear that, in a 4-rod cluster, the wall effects of the shroud have a strong influence, too. It should be pointed out that all the data presented in these figures gives only a qualitative idea of how design and flow characteristics can influence the critical heat flux.

In the literature, more and more burnout measurements can be found that were done not with water but with a modeling fluid; for example, with Freon. Tests with modeling fluid usually are performed because the test objects as well as the test itself are much cheaper than with water. Furthermore, modeling fluids, due to their lower boiling pressure and temperature, are more convenient to handle. The answer to the question of how these test results can be transformed to water conditions is disclosed several times in detail in the literature (Barnett, 1965; Stevens and Macbeth, 1970; and Behar et al., 1969). The scaling laws reported there give a fixed factor for mass flow-rate transformation, but more recent studies (Hein and Kastner, 1972) showed that there should be a correction factor varying with mass flow rates. In Fig. 10 it is shown clearly that with a constant transforming factor F_q, as worked out by Behar et al. (1969) the agreement of measurements in Freon 12 (solid black circles), which are already scaled to water conditions, with water data (open squares) worked out with the same test section is moderately good. There can be seen a strong tendency of the deviation with mass flow rate. A simple mass flow correction, $(\dot{m}/\dot{m}_K)^{0.13}$, gives almost complete agreement (open circles).

This correction also works quite satisfactorily in radial nonuniform heat flux distribution, up to very high hot-channel factors, as Fig. 11 demonstrates. The correction has not been applied in the results shown there, but it can be seen that it will work as well as before.

5 CRITICAL HEAT FLUX IN TRANSIENT CONDITIONS

For emergency cases as, for example, when the pumps cease operation, or when a control rod drops, the behavior of the critical heat flux under special transient conditions, especially for mass flow-rate diminutions and for power excursions, is of interest.

In the literature, there are several measurements that deal with power excursions in test sections of very simple geometry, such as wires and strips, but only a few tests with reactor-like rod bundles were performed (Hein and Kastner, 1972; Moxon and Edwards, 1967).

From the safety point of view, the question arises as to whether higher critical heat fluxes can be achieved under transient conditions than in steady state, always referred to the same hydro- and thermodynamic parameters, i.e., can the transient critical heat flux be predicted by the usual burnout correlations making quasisteady assumptions?

One has to realize that it takes a certain time until nucleate boiling changes to film boiling, or until the dry patch is formed, when the critical heat flux is reached. With fast power excursions, complex flow conditions will be created

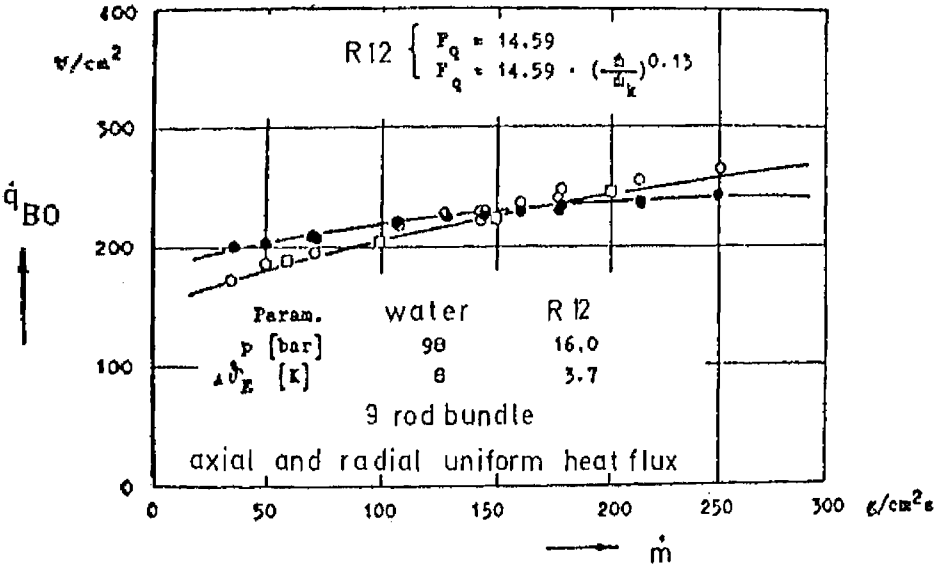

FIG. 10 Scaling of test results carried out in Freon to water conditions; correction factor to Bouré's scaling law.

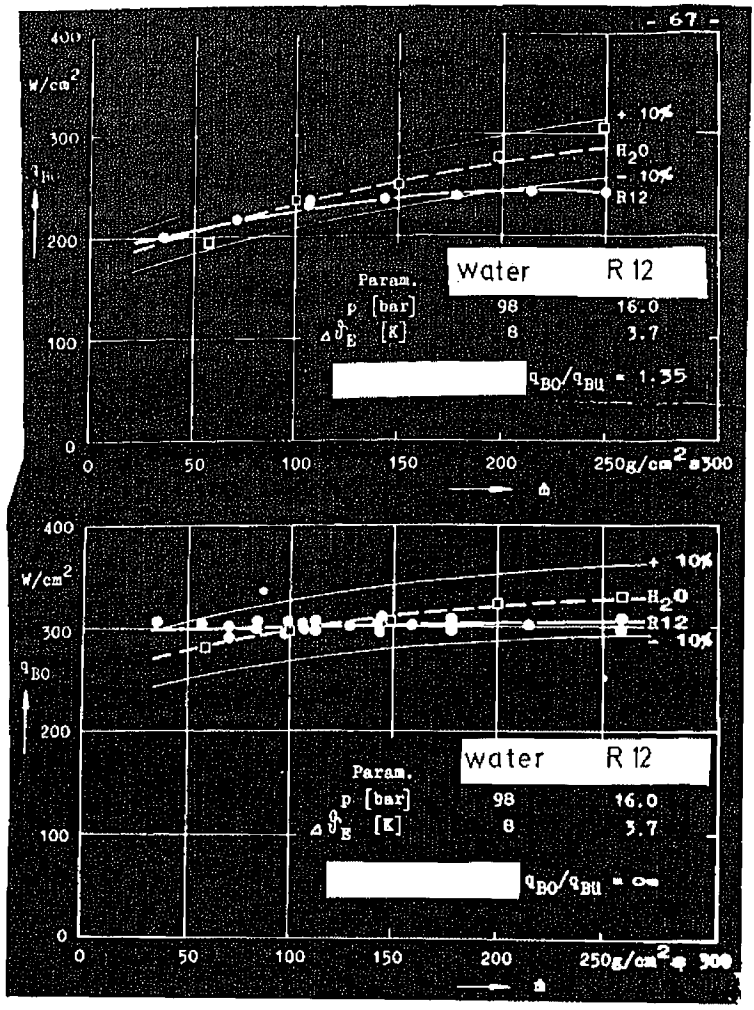

FIG. 11 Scaling of Freon data to water conditions with radial nonuniform power distribution.

in forced convection. The boundary layer at the heated wall changes, there is a strong acceleration of the fluid due to additional evaporation, and it takes some time until the higher quality produced in the liquid along the rods reaches the downstream burnout spot. All these effects tend to improve the heat transfer and retard the achievement of higher heat fluxes, the faster and steeper the transient occurs. That this is true can clearly be seen from Fig. 12, where the ratio of the critical heat flux reached under transient conditions to the critical heat flux under steady-state conditions is plotted versus the time of power excursion; that is, the time in which the power was raised from zero to critical heat flux. With very rapid transients, improvements up to a factor of 2 were found.

In rod clusters, there are many other influences in addition to the steepness

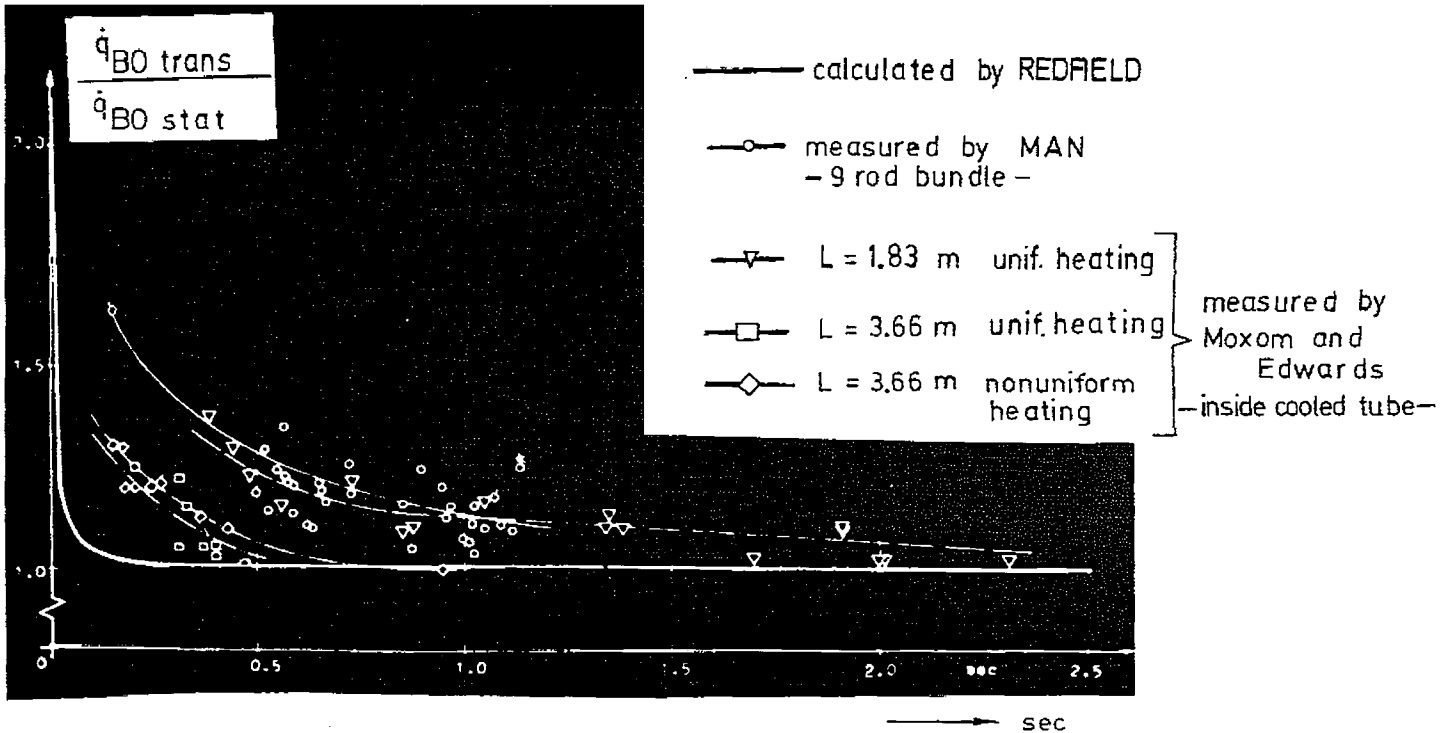

FIG. 12 Influence of duration of transient on the critical flux comparison of diverse measured and calculated values.

of the transient ramp. The more "slender" the cooling channel, i.e., the subassembly of the rod bundle, the higher the acceleration of the fluid. Radial nonuniform heat flux distribution makes mixing phenomena effective and competitive with power excursion and fluid acceleration. A qualitative comparison of these influences and effects is shown in Fig. 13. The diagonally hatched fields give the comparison if hydro- and thermodynamic conditions at the inlet of the test section are used as reference parameters, and the cross-hatched fields are valid for identical outlet conditions. Comparing these results leaves many open questions, but they do give general qualitative information.

More quantitative data are presented in Fig. 14. These tests were done with an axial and radial uniformly heated 4-rod cluster. Test fluid was Freon.

Generally one can say, that it is certainly conservative, when in the safety analysis of power excursion burnout correlations are used, which are proved for steady-state conditions. Loss of flow transients due to a pump failure are

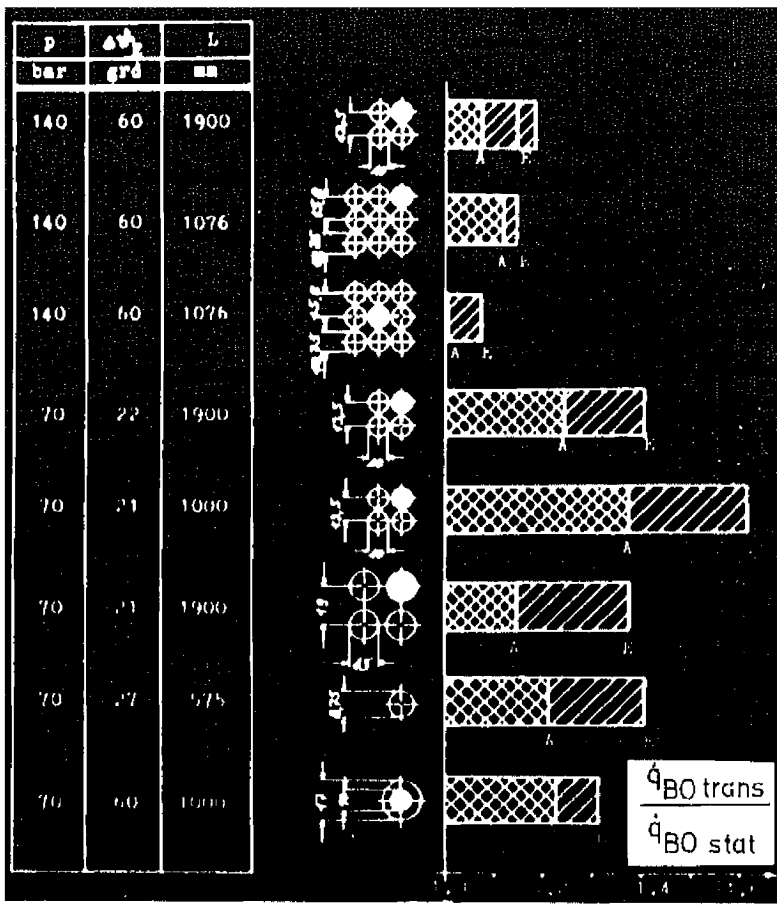

FIG. 13 Influence of the slenderness of the cooling channel on transient critical heat flux with power excursions.

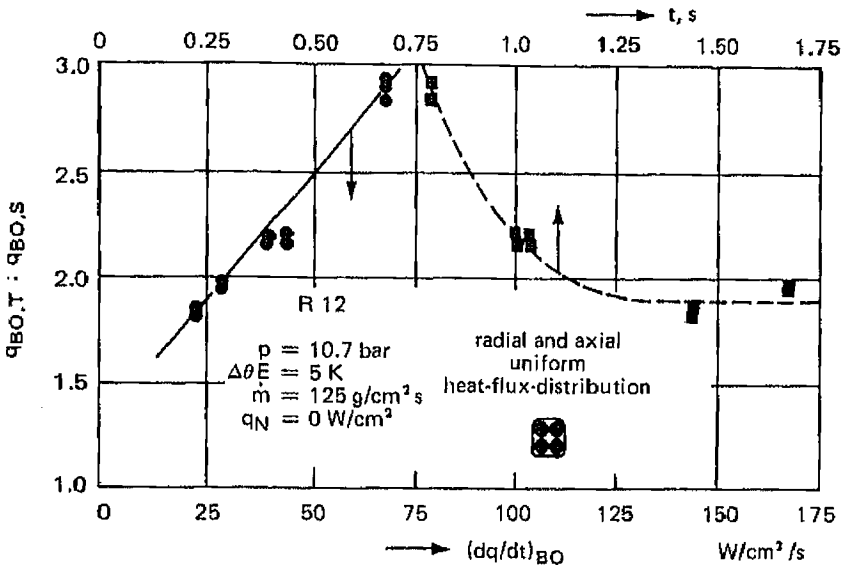

FIG. 14 Influence of the changing velocity of the heat-flux density on burnout behavior with power transients in a 4-rod cluster.

much slower than power excursions, therefore, almost no change with respect to steady-state conditions is to be expected. This is proved by measurements (Hein and Kastner, 1972), as shown in Figs. 15 and 16.

The tests were performed as follows: from a given steady state, with a certain mass flow rate and heat flux, the mass flow rate in the rod bundle was lowered continuously until burnout occurred; the heat flux was kept constant, as shown by the horizontal lines in these figures. In addition, results also are plotted under pure steady-state conditions (open circles). One can see that the results of the loss-of-flow tests (solid black circles) and of the steady-state tests fall within the same curve. The basis of this comparison is that the local (at the burnout spot) and temporal thermo- and hydrodynamic conditions are the same in both conditions. These results show that the burnout behavior during a pump failure can be predicted in a straightforward manner by burnout correlations with quasisteady assumptions.

It should be mentioned that in a real loss-of-flow accident, the power drops down immediately due to a scram and, therefore, the tests discussed above were not fully realistic. Also, tests simulating these conditions gave the same results, as the two examples in Fig. 16 demonstrate. Here, using time as the abcissa, the mass flow rate and the heat flux are plotted for two tests. In addition, a curve for the critical heat flux is drawn in as it results from a burnout correlation, assuming quasisteady-state conditions. The critical heat flux observed in the tests is marked with a circle and the index "BO." In the

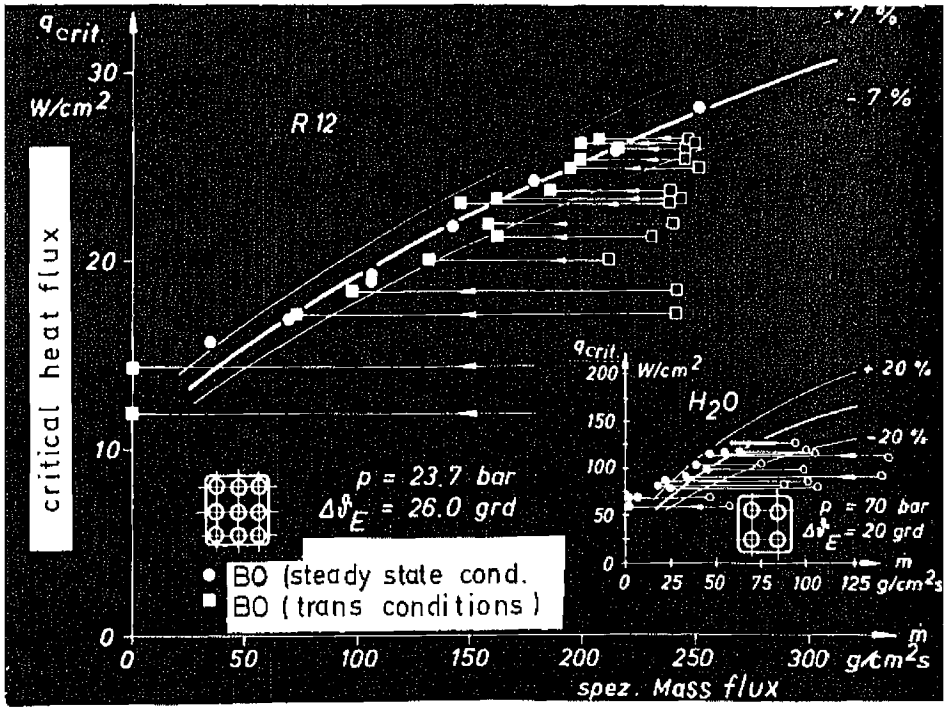

FIG. 15 Critical heat flux under mass-flow transients in Freon 12, 9-rod cluster, power constant. *Inset*: Critical heat flux under mass-flow transients, 4-rod cluster, power constant.

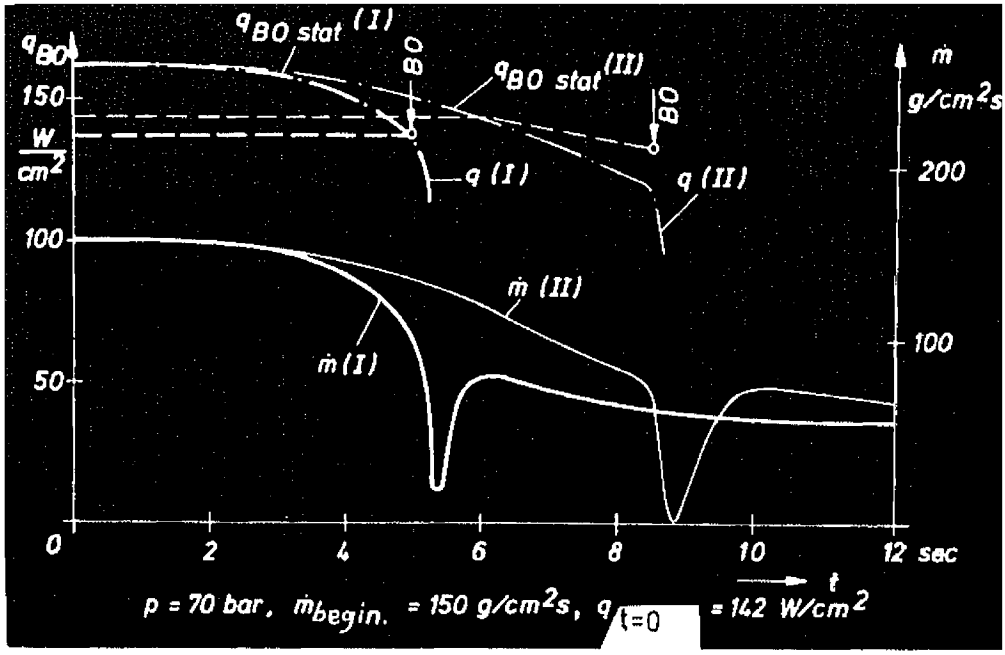

FIG. 16 Combined mass flow and power transients.

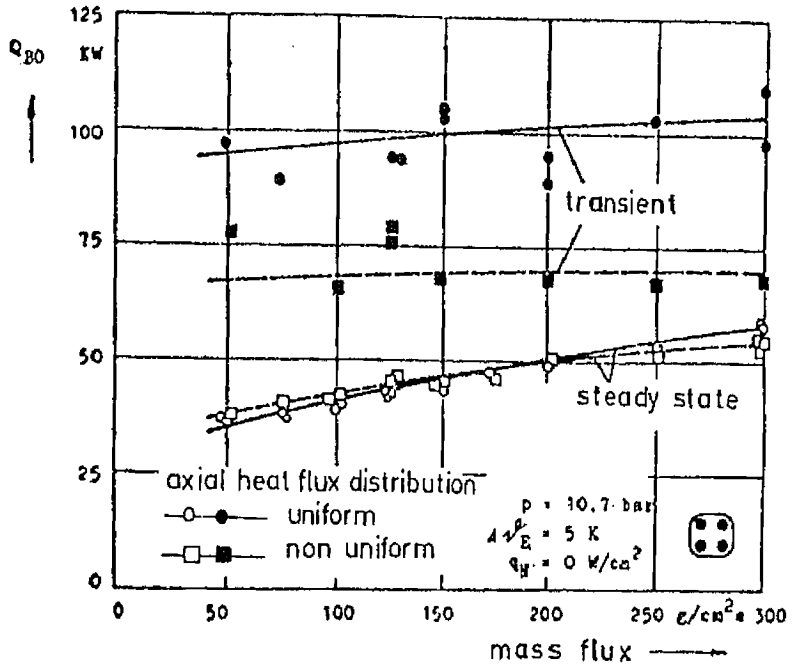

FIG. 17 The use of the overall power hypothesis for steady-state and transient critical heat flux.

first test, the heat flux was not lowered and there is full agreement between correlation and measurement. In the second test, the heat flux was reduced slightly and here the prediction is conservative.

All the transient tests discussed up to now were done with axial uniform heat-flux distribution. The question is how to predict the behavior with nonuniform heat flux. The simplest way would be to use the overall power hypothesis as mentioned briefly in Chap. 2 and discussed in detail by Hewitt (1966). The hypothesis assumes that the critical power is the same with uniform and nonuniform heating. While this assumption works quite well in steady-state conditions for the test series shown in Fig. 17, it fails completely for power excursions. The reason is very simple: the critical heat flux with power excursions is strongly affected by the acceleration of the fluid in the test section due to additional evaporation, and this is a "flow history" effect, which is not taken into account in the overall power hypothesis.

REFERENCES

Anderson, P. S. (1972). Developing Film Flow: An Analysis of Adiabatic Data and a New Model for Diabatic Flow, Riso Report *SDS*-50.

Barnett, P. G. (1964). The Prediction of Burnout in Nonuniformly Heated Rod Clusters From Burnout Data for Uniformly Heated Round Tubes, *AEEW-R* 362.

Barnett, P. G. (1965). Scaling of Burnout in Forced Convection Boiling Heat Transfer, *Proc. Inst. Mech. Eng.*, vol. 180, pt. 30, *Paper* 15.

Behar, M., Bouré, J., Courtaud, M., and Rieque, R. (1969). Similitude des Ecoulements Diphasiques Liquidevapeur, avec Echanges de Chaleur, Centre d'Etudes Nucleaires de Grenoble, Service des Transferts Thermiques, Rapport T.T. no. 91.

Biancone, F. et al. (1965). Forced Convection Burnout and Hydrodynamic Instability Experiments for Water at High Pressure, pt. I, *EUR* 2490e.

Collier, J. G. (1972). "Convective Boiling and Condensation," McGraw-Hill Book Co., London.

Hein, D., and Kastner, W. (1972). Versuche zur kritischen Heizflächenbelastung unter stationären und instationären Bedingungen in Frigen 12 und Wasser, Teil 1, M.A.N.-Bericht no. 45.03.02.

Hewitt, G. F., Bennett, A. W., et al. (1966). Studies of Burnout in Boiling Heat Transfer to Water in Round Tubes with Nonuniform Heating, *AERE-R* 5076.

Hutchinson, P., Whalley, P. B., and Hewitt, G. F. (1973). Transient Flow Redistribution in Annular Two-Phase Flow, *Paper 26, Int. Meeting on Reactor Heat Transfer*, Karlsruhe.

Lee, D. H. (1965). An Experimental Investigation of Forced Convection Burnout in High Pressure Water, pt. III, *AEEW-R* 355.

Lee, D. H. (1966). An Experimental Investigation of Forced Convection Burnout in High Pressure Water, pt. IV, *AEEW-R* 479.

Lee, D. H., and Obertelli, J. D. (1963). An Experimental Investigation of Forced Convection Burnout in High Pressure Water, pt. II, *AEEW-R* 309.

Macbeth, R. V. (1963). Burnout Analysis, pt. 4: Application of Local Condition Hypothesis to World Data for Uniformly Heated Round Tubes and Rectangular Channels, *AEEW-R* 267.

Moxon, D., and Edwards, P. A. (1967). Dryout During Flow and Power Transients, *European Two-Phase Heat-Transfer Meeting*, Bournemouth, also *AEEW-R* 553.

Silvestri, M. (1966). On the Burnout Equation and on Location of Burnout Points, *Energia Nucleare*, vol. 13, no. 9, pp. 469–479.

Smith, D. G., Tong, L. S., and Rohner, W. M. (1965). Burnout in Steam-Water Flows with Axial Non-Uniform Heat Flux, *ASME Paper* 65-*WA/HT*-33.

Stevens, G. F., and Macbeth, R. V. (1970). The Use of Freon 12 to Model Forced Convection Burnout in Water: The Restriction on the Size of the Model, *ASME Paper* 70-*HT*-20.

Sursock, J. P. (1973). Dryout Model in Two-Phase Flow, *CEA* Report *CEA-N*-1665.

Swenson, H. S. et al. (1964). Non-Uniform Heat Generation Experimental Programme *Q PR* no. 4, 5, 6, 7, and 8 (*BAW*-3238).

Todreas, N. E., and Rohsenow, W. M. (1965). The Effect of Nonuniform Axial Heat-Flux Distribution, MIT-9843-37, see also Paper 89, *1966 Int. Heat Transfer Conf.*, Chicago.

Tong, L. S. (1965). "Boiling Heat Transfer and Two-Phase Flow," John Wiley & Sons, Inc., New York.

Tong, L. S. (1966). Prediction of Departure From Nucleate Boiling for an Axially Non-Uniform Heat Flux Distribution, *WCAP*-5584 Rev. 1; see also *J. Nucl. Energy*, vol. 21, no. 3, pp. 241–248, (1967).

Tong, L. S., Lurrin, H. B., Larsen, P. S., and Smith, O. G. (1966). Influence of Axial Non-Uniform Heat Flux on DNB, *Chem. Eng. Progr., Symp. Ser., Heat Transfer*, Los Angeles, vol. 62, no. 64, pp. 35–40; also *WCAP*-2767 (1965).

Whalley, P. B., Hutchinson, P., and Hewitt, G. F. (1973). The Calculation of Critical Heat Flux in Forced Convective Boiling, *Paper* 84, *European Two-Phase Flow Group Meeting*, Brussels.